KEAP1/NFE2L2 Mutations Predict Lung Cancer Radiation Resistance That Can Be Targeted by Glutaminase Inhibition

Michael S. Binkley[1], Young-Jun Jeon[2,3], Monica Nesselbush[4], Everett J. Moding[1], Barzin Y. Nabet[1,2], Diego Almanza[4], Christian Kunder[5], Henning Stehr[5], Christopher H. Yoo[1], Siyeon Rhee[6], Michael Xiang[7], Jacob J. Chabon[2], Emily Hamilton[4], David M. Kurtz[8], Linda Gojenola[5], Susie Grant Owen[1], Ryan B. Ko[1], June Ho Shin[2], Peter G. Maxim[1], Natalie S. Lui[9], Leah M. Backhus[9], Mark F. Berry[9], Joseph B. Shrager[9], Kavitha J. Ramchandran[2,8], Sukhmani K. Padda[2,8], Millie Das[2,8], Joel W. Neal[2,8], Heather A. Wakelee[2,8], Ash A. Alizadeh[2,8], Billy W. Loo Jr[1,2], and Maximilian Diehn[1,2,10]

ABSTRACT

Tumor genotyping is not routinely performed in localized non–small cell lung cancer (NSCLC) due to lack of associations of mutations with outcome. Here, we analyze 232 consecutive patients with localized NSCLC and demonstrate that *KEAP1* and *NFE2L2* mutations are predictive of high rates of local recurrence (LR) after radiotherapy but not surgery. Half of LRs occurred in tumors with *KEAP1/NFE2L2* mutations, indicating that they are major molecular drivers of clinical radioresistance. Next, we functionally evaluate *KEAP1/NFE2L2* mutations in our radiotherapy cohort and demonstrate that only pathogenic mutations are associated with radioresistance. Furthermore, expression of NFE2L2 target genes does not predict LR, underscoring the utility of tumor genotyping. Finally, we show that glutaminase inhibition preferentially radiosensitizes *KEAP1*-mutant cells via depletion of glutathione and increased radiation-induced DNA damage. Our findings suggest that genotyping for *KEAP1/NFE2L2* mutations could facilitate treatment personalization and provide a potential strategy for overcoming radioresistance conferred by these mutations.

SIGNIFICANCE: This study shows that mutations in *KEAP1* and *NFE2L2* predict for LR after radiotherapy but not surgery in patients with NSCLC. Approximately half of all LRs are associated with these mutations and glutaminase inhibition may allow personalized radiosensitization of *KEAP1/NFE2L2*-mutant tumors.

INTRODUCTION

More than 40% of patients with lung cancer are diagnosed with localized disease and are potential candidates for curative treatment (1). For stage III non–small cell lung cancer (NSCLC), concurrent chemoradiotherapy (CRT) with conventionally fractionated radiotherapy (RT) is a mainstay of treatment. Although distant recurrence is the most common pattern of failure, ~30% of patients experience local recurrence (LR), which is associated with worse overall survival

[1]Department of Radiation Oncology, Stanford University, Stanford, California. [2]Stanford Cancer Institute, Stanford, California. [3]Department of Integrative Biotechnology, Sungkyunkwan University, Suwon, Republic of Korea. [4]Cancer Biology Program, Stanford University, Stanford, California. [5]Department of Pathology, Stanford University, Stanford, California. [6]Department of Biology, Stanford University, Stanford, California. [7]Department of Radiation Oncology, University of California, Los Angeles, Los Angeles, California. [8]Division of Oncology, Department of Medicine, Stanford University, Stanford, California. [9]Division of Thoracic Surgery, Department of Cardiothoracic Surgery, Stanford University School of Medicine, Stanford, California. [10]Institute for Stem Cell Biology and Regenerative Medicine, Stanford University, Stanford, California.

Note: Supplementary data for this article are available at Cancer Discovery Online (http://cancerdiscovery.aacrjournals.org/).

M.S. Binkley and Y.-J. Jeon contributed equally to this article.

Current address for P.G. Maxim: Department of Radiation Oncology, Indiana University School of Medicine, Indianapolis, IN.

Corresponding Author: Maximilian Diehn, Stanford University, 875 Blake Wilbur Drive, Stanford, CA 94305-5847. Phone: 650-721-1550; Fax: 650-723-3913; E-mail: diehn@stanford.edu

Cancer Discov 2020;10:1826–41

doi: 10.1158/2159-8290.CD-20-0282

(OS; refs. 2, 3). For patients with stage I–II NSCLC who are not candidates for surgery, stereotactic ablative radiotherapy (SABR) is the preferred treatment and is associated with ~90% local control (4, 5). For NSCLC treated by CRT or SABR, tumor burden is the only variable that has been repeatedly associated with risk of LR (6–10).

Although somatic mutations play a critical role in personalizing systemic therapy in advanced NSCLC, this is not the case for patients undergoing RT. Recently, mutations in several genes have been suggested to be associated with clinical LR, but these findings remain preliminary and not validated (11–13). Mutations leading to activation of the KEAP1–NFE2L2 pathway are particularly promising candidates for contributing to clinical radioresistance because NFE2L2 is a transcription factor that drives expression of free radical defense genes which could interfere with radiation-induced DNA damage. KEAP1 is an adaptor protein that targets NFE2L2 for ubiquitination and proteasomal destruction under normal homeostasis (14). Mutations in *KEAP1* or *NFE2L2* occur in approximately 20% of NSCLC (15, 16) and lead to constitutive activation of the pathway. Previous studies have demonstrated that activation of the pathway *in vitro* (14, 17–19) or *in vivo* promotes radioresistance (17). Furthermore, our group previously reported an association of *KEAP1/NFE2L2* mutations with high risk of LR in a heterogeneous pilot cohort of patients with localized NSCLC treated with RT (17).

In the current study, we sought to identify recurrent mutations in localized NSCLC that are associated with LR after RT. We found that *KEAP1/NFE2L2* mutations strongly increase the risk of LR after RT but not surgery. Functional classification of mutations using isogenic cell line systems to distinguish pathogenic and passenger mutations further strengthened the association of mutations with LR. Finally, we demonstrate that glutaminase inhibition is a potential approach for personalized radiosensitization of *KEAP1/NFE2L2*-mutant tumors.

RESULTS

KEAP1/NFE2L2 Mutations Are Predictive Biomarkers of LR after RT

We identified 232 consecutive patients who were treated at Stanford University with curative intent with RT or surgery and who underwent tumor genotyping using a clinical hybrid capture–based sequencing assay covering 130 to 198 genes (20). Our study included three cohorts: (i) 47 patients with locally advanced NSCLC treated with conventionally fractionated RT (CRT cohort), (ii) 50 patients with early-stage NSCLC treated with high-dose SABR (SABR cohort), and (iii) 135 patients with early-stage NSCLC treated with surgical resection (surgery cohort; Fig. 1A). None of these were included in our previously published cohort of RT-treated patients with *KEAP1/NFE2L2* tumor genotyping (17). Differences in baseline patient characteristics were reflective of the types of patients routinely selected for each type of treatment (Supplementary Table S1).

In order to identify tumor mutations associated with clinical radioresistance, we determined the association between recurrent mutations and LR in the combined cohort of patients treated with CRT or SABR. LR, defined as tumor regrowth within the radiation field, was chosen as the endpoint of interest because it is most likely to reflect responses of tumor cells exposed to RT. Distant recurrence outside of the prior radiation field could be due to micrometastases that were present at the time of treatment and that were therefore not exposed to RT. Ten mutations met our predetermined recurrence frequency threshold of >5% (Fig. 1B; see Methods for power calculation). Mutations in *KEAP1* and *NFE2L2* were considered as one group because they result in the same biochemical phenotype (i.e., NFE2L2 overexpression) and display mutual exclusivity (14, 17). Strikingly, only *KEAP1/NFE2L2* mutations were significantly associated with LR (Fig. 1C; adjusted $P = 0.005$), and these mutations were present in nearly half of tumors that had LR (Fig. 1D). Mutations in *KEAP1* were distributed throughout the protein, whereas *NFE2L2* mutations were located in the DLG and ETGE hotspots (Fig. 1E). Furthermore, in exploratory analyses, we found that *KEAP1* mutations were significantly associated with LR on their own ($P = 0.002$) and that neither mutations leading to ERK activation (*EGFR/KRAS/BRAF*; $P = 0.49$) nor E2F activation (*CDKN2A/RB1*; $P = 0.15$) were associated with LR when considered together. The frequency of comutations in driver genes was similar in *KEAP1/NFE2L2*-mutant tumors with and without LR (5 of 7 with LR vs. 4 of 10 without LR; $P = 0.33$). We also did not observe a significantly different frequency of co-occurring *TP53* mutations in *KEAP1/NFE2L2*-mutant tumors with (3 of 7) versus without LR (8 of 10; $P = 0.16$; Fig. 1B). Thus, among recurrent mutations in NSCLC, *KEAP1/NFE2L2* mutations appear to be the dominant cause of clinical radioresistance.

Next, we compared LR based on *KEAP1/NFE2L2* mutation status in patients with locally advanced NSCLC treated with conventionally fractionated CRT. For the entire CRT cohort, 2-year OS was 65.6% [95% confidence interval (CI), 46.9%–79.1%] and 2-year LR was 22.8% (95% CI, 20.8%–24.8%; Supplementary Fig. S1A and S1B), similar to the rates reported for the standard RT dose arm in RTOG 0617 (21). Patients with *KEAP1/NFE2L2*-mutant tumors had a significantly increased incidence of LR compared with those without, with 2-year LR of 50.0% (95% CI, 36.3%–63.7%) versus 16.9% (95% CI, 14.6%–19.2%), respectively ($P = 0.01$; Fig. 1F). There were no significant differences in clinical characteristics between *KEAP1/NFE2L2*^{MUT} and wild-type (WT) cases (Supplementary Table S2). Metabolic tumor volume (MTV) measured using FDG PET/CT scans and stage did not differ significantly between patients with and without *KEAP1/NFE2L2* mutations ($P = 0.45$ and $P = 0.67$, respectively). Furthermore, *KEAP1/NFE2L2* mutation status was the only predictor of LR in both univariable analysis (UVA; HR = 4.74; 95% CI, 1.30–17.20; $P = 0.02$) and multivariable analysis (MVA; HR = 5.17; 95% CI, 1.30–20.58; $P = 0.02$; Supplementary Table S3). We did not observe a significant association between *KEAP1/NFE2L2* mutations and distant recurrence as first recurrence after CRT ($P = 0.69$; Supplementary Table S4 and Supplementary Fig. S1C), suggesting that patients with locally advanced NSCLC and *KEAP1/NFE2L2* mutations are specifically at high risk of LR.

Patients with stage I–II NSCLC treated with hypofractionated SABR receive significantly higher radiation doses than patients treated with conventionally fractionated CRT.

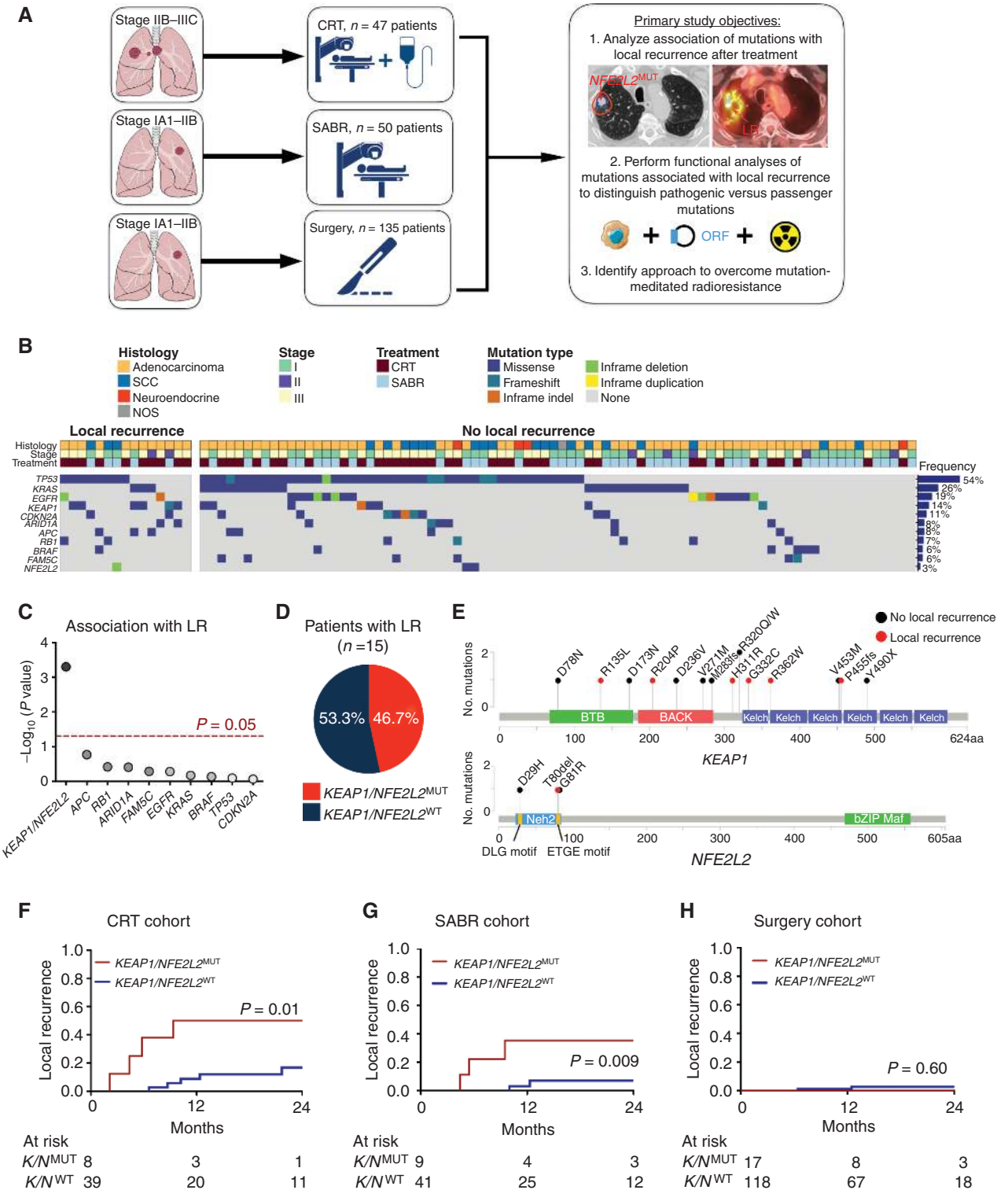

Figure 1. *KEAP1/NFE2L2* mutations are predictive biomarkers of LR after RT. **A,** Study design (images were produced and modified from Servier Medical Art; see Acknowledgments). **B,** Recurrent mutations in patients with and without LR after CRT or SABR. NOS, not otherwise specified; SCC, squamous cell carcinoma. **C,** Association of recurrent mutations with LR. Competing risk comparison performed using Gray test with multiple hypothesis testing correction. **D,** Pie chart fraction of LR events occurring in tumors with *KEAP1* or *NFE2L2* mutations. **E,** Location of *KEAP1* and *NFE2L2* mutations from CRT and SABR cohorts. **F,** Incidence of LR stratified by *KEAP1/NFE2L2* mutation status for patients with stage IIB–IIIC NSCLC receiving CRT. **G,** Incidence of LR stratified by *KEAP1/NFE2L2* mutation status for patients with stage IA1–IIB NSCLC treated with SABR. **H,** Incidence of LR stratified by *KEAP1/NFE2L2* mutation status for patients with stage IA1–IIB NSCLC treated with surgical resection.

We therefore assessed whether the "ablative" doses delivered during SABR might overcome *KEAP1/NFE2L2* mutation–associated radioresistance. Patients in the SABR cohort had 2-year OS of 82.8% (95% CI, 68.5%–91.0%) and 2-year LR of 12.4% (95% CI, 10.9%–13.9%; Supplementary Fig. S2A and S2B). Surprisingly, as in the CRT cohort, we observed a significantly higher incidence of LR after high-dose SABR for patients with *KEAP1/NFE2L2* mutations versus those without, with 2-year LR of 35.2% (95% CI, 23.5%–46.9%) versus 7.0% (95% CI, 5.6%–8.4%), respectively (Fig. 1G; $P = 0.009$). There were no significant differences in clinical characteristics between *KEAP1/NFE2L2*^{MUT} and wild-type cases (Supplementary Table S2). MTV and stage were not significantly different between patients with and without *KEAP1/NFE2L2* mutations ($P = 0.88$ and $P = 0.71$, respectively). On both UVA and MVA, *KEAP1/NFE2L2* mutations (HR = 8.50; 95% CI, 1.56–46.30; $P = 0.01$ and HR = 17.92; 95% CI, 2.05–156.67; $P = 0.009$, respectively) and MTV (HR = 1.42 per 10 cc; 95% CI, 1.25–1.62; $P = 1.2e{-}7$ and HR = 1.68; 95% CI, 1.27–2.22; $P = 0.0003$, respectively) were significantly associated with LR (Supplementary Table S3). We did not observe a significant association between *KEAP1/NFE2L2* mutations and distant recurrence as first recurrence after SABR ($P = 0.17$; Supplementary Table S5 and Supplementary Fig. S2C). Thus, *KEAP1/NFE2L2* mutations are predictive of LR after SABR.

Lastly, we hypothesized that *KEAP1/NFE2L2* mutations are not associated with LR after surgery, because the expression of free radical defense genes induced by these mutations would not be expected to affect tumor resectability. In our 135-patient surgery cohort, LR at the staple line or bronchial stump was a rare occurrence (1- and 2-year rates of 0.9 and 2.3%, respectively) and, consistent with our hypothesis, did not differ based on *KEAP1/NFE2L2* mutation status (Fig. 1H). There were no significant differences in patient age and tumor size between *KEAP1/NFE2L2*^{MUT} and wild-type cases, but mutant cases were more likely to have non-adenocarcinoma histology and a more significant smoking history (Supplementary Table S2). Our findings are consistent with prior reports showing that LR is not a primary pattern of failure after surgery (22). Additionally, we validated there is no difference in prognosis by mutation status within patients with stage I–II lung adenocarcinoma and squamous cell carcinoma treated with primary surgery in The Cancer Genome Atlas (TCGA; $P = 0.71$; Supplementary Fig. S3). Taken together, our results indicate that *KEAP1/NFE2L2* mutations are predictive biomarkers for LR after RT but not surgery.

Functional Evaluation of *KEAP1/NFE2L2* Mutations

Although our clinical results indicate that *KEAP1/NFE2L2* mutations are strongly associated with LR after RT, 58.8% (10 of 17) of patients with these mutations did not develop tumor regrowth within the radiation field. We therefore hypothesized that a subset of the mutations were passengers that did not affect protein function. To test this hypothesis, we developed isogenic *KEAP1* wild-type and knockout cell lines in which we could express open reading frame (ORF) constructs containing the mutations we observed in the two RT cohorts and functionally evaluated these for KEAP1/NFE2L2 pathway activity (Fig. 2A). Specifically, we targeted *KEAP1* in H1299 human NSCLC cells using CRISPR/Cas9-mediated gene editing by directly introducing the single guide RNA (sgRNA)–Cas9 complex (Supplementary Fig. S4A and S4B; ref. 23). *KEAP1*^{NULL} H1299 cells displayed significant overexpression of NFE2L2 and its targets, including NQO1 and SQSTM1 (also known as p62), compared with parental *KEAP1*^{WT} H1299 cells (Fig. 2B). Additionally, these cells displayed significant resistance to ionizing radiation (Fig. 2C).

To explore the mechanism of radiation resistance induced by *KEAP1* loss, we next examined levels of DNA damage induced by ionizing radiation in the isogenic lines. Although baseline levels of DNA double-strand breaks as measured by γH2AX foci were similar, there were significantly fewer foci in *KEAP1*^{NULL} compared with *KEAP1*^{WT} H1299 cells following 2 Gy of ionizing radiation (Fig. 2D). These findings suggest that *KEAP1*^{NULL} cells are radioresistant due to elevated levels of free radical scavengers and decreased DNA damage production by the indirect effect of ionizing radiation. To test this hypothesis, we examined levels of glutathione (GSH) and found that *KEAP1*^{NULL} H1299 cells had significantly higher levels of reduced GSH than *KEAP1*^{WT} cells (Supplementary Fig. S4C). Next, we examined the effects of the free radical scavenger N-acetylcysteine (NAC) and the GSH biosynthesis inhibitor buthionine sulfoximine (BSO) on radiation sensitivity. Although treatment with NAC had no effect in unirradiated cells, it significantly enhanced survival of *KEAP1*^{WT} but not *KEAP1*^{NULL} H1299 cells after 4 Gy, suggesting that *KEAP1*^{NULL} H1299 cells are already maximally protected by endogenous free radical scavengers (Fig. 2E). Conversely, BSO treatment had no effect on radiosensitivity of *KEAP1*^{WT} cells but radiosensitized *KEAP1*^{NULL} cells to levels similar to those of *KEAP1*^{WT} cells. These data suggest that elevated levels of GSH are a major driver of the radioresistant phenotype of *KEAP1*^{NULL} cells.

In order to evaluate the functional effects of the *KEAP1* mutations we observed in the RT patients, we individually expressed ORFs carrying the 15 *KEAP1* mutations in *KEAP1*^{NULL} H1299 cells and tested multiple aspects of KEAP1/NFE2L2 pathway activity. We reasoned that pathogenic (i.e., inactivating) mutations should maintain KEAP1/NFE2L2 pathway activity, whereas passenger mutations should act like wild-type KEAP1 and decrease it. We first confirmed that expression levels of both mutant and wild-type KEAP1 constructs were similar (Supplementary Fig. S5A). Next, we analyzed expression of the NFE2L2 target gene *HMOX1* by qRT-PCR and observed that all 6 constructs containing *KEAP1* mutations from LR cases did not alter expression, consistent with a loss-of-function phenotype (Fig. 2F). Conversely, 6 of 9 (67%) constructs containing mutations from non-LR cases decreased expression similarly to wild-type KEAP1, suggesting that these mutations do not alter KEAP1 function. Similar results were observed when examining expression of HMOX1 and SQSTM1 at the protein level (Supplementary Fig. S5B–S5F). Furthermore, we performed *in vitro* clonogenic survival assays using 5 Gy of ionizing radiation and observed that all 6 constructs containing *KEAP1* mutations from LR cases did not resensitize *KEAP1*^{NULL} H1299 cells, whereas 6 of 9 (67%) constructs containing mutations from non-LR cases did (Fig. 2G). Finally, we observed the same pattern when examining resistance to hydrogen peroxide (Supplementary Fig. S5G).

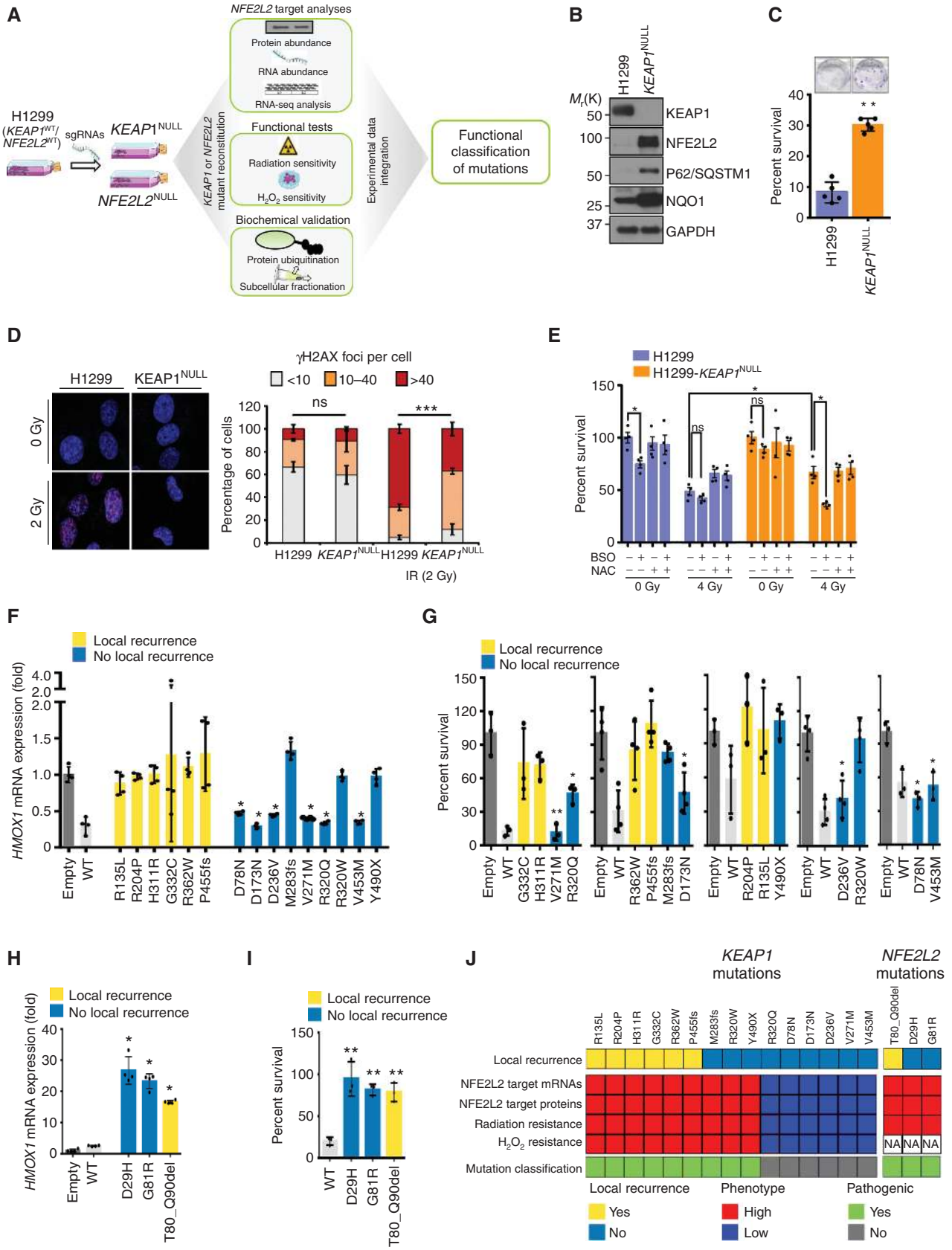

In an analogous fashion, we developed isogenic *NFE2L2* wild-type and knockout cell lines. *NFE2L2*^{NULL} H1299 cells displayed loss of NFE2L2 protein, reduced target gene expression, and greater sensitivity to ionizing radiation compared with parental *NFE2L2*^{WT} H1299 cells (Supplementary Fig. S6A and S6B). We expressed ORFs carrying each of the three *NFE2L2* mutations from our RT cohorts in *NFE2L2*^{NULL} H1299 cells (Supplementary Fig. S6C and S6D). To remove any native NFE2L2, we generated a KEAP1 overexpression cell model using the *NFE2L2*^{NULL} H1299 cells transfected with multiple copies of wild-type *KEAP1* (Supplementary Fig. S6D). Although wild-type *NFE2L2* did not significantly increase NFE2L2 target gene expression, each of the three mutant constructs did, suggesting KEAP1-mediated degradation of wild-type but not mutant NFE2L2 (Fig. 2G). Analysis of protein expression of NFE2L2 and targets HMOX1 and GCLM confirmed stabilization of the mutant but not wild-type NFE2L2 constructs (Supplementary Fig. S6D). Finally, all 3 mutant but not wild-type *NFE2L2* constructs induced increased protein expression of HMOX1 (Fig. 2H) and resistance to ionizing radiation and hydrogen peroxide in *NFE2L2*^{NULL} H1299 cells (Fig. 2I; Supplementary Fig. S6E). Figure 2J provides a summary of functional assay results and mutation classification for each *KEAP1* and *NFE2L2* mutation found in the CRT and SABR cohorts.

Functional Classification of *KEAP1/NFE2L2* Mutations Improves the Association with LR

Based on these molecular analyses, we classified the *KEAP1* and *NFE2L2* mutations observed in our RT cohorts as either pathogenic (i.e., loss-of-function for *KEAP1* or gain-of-function for *NFE2L2*) or passenger (i.e., neutral). For *KEAP1*, 9 of 15 (60%) mutations were pathogenic, whereas 6 (40%) were passengers, and for *NFE2L2*, all 3 mutations were pathogenic (Fig. 2I). Notably, we observed LR only in patients with pathogenic *KEAP1* or *NFE2L2* mutations and in none of the patients with passenger mutations (Fig. 3A). Additionally, we found that patients with pathogenic mutations who did not develop LR had significantly smaller tumors (median 2.7 cc) than those who did develop LR (median 64.1 cc; $P = 0.03$; Fig. 3B). Among patients with pathogenic mutations, 28.6% (2 of 7) with tumors <20.4 cc experienced an LR, whereas 100% (5 of 5) with tumors ≥20.4 cc experienced an LR. These findings suggest that doses of RT delivered during CRT or SABR can control some tumors carrying pathogenic mutations if tumors are small and fewer clonogens are present.

Reanalyzing LR rates in CRT- and SABR-treated patients based on the presence of pathogenic mutations increased separation between mutant and wild-type patients (Supplementary Fig. S7A and S7B). Strikingly, rates of LR did not differ significantly between patients treated with CRT or SABR when mutation functional classification was considered (Fig. 3C; $P = 0.54$). Patients with pathogenic *KEAP1/NFE2L2* mutations who were treated with SABR had a significantly worse OS than nonmutant patients (Fig. 3D; $P = 0.002$). Similarly, the presence of *KEAP1/NFE2L2* mutations was associated with inferior survival in patients with stage I–IIA NSCLC from TCGA who were treated with radiation and not surgery (Fig. 3E; $P = 0.01$; ref. 24). Thus, functional classification of *KEAP1/NFE2L2* mutations improves their association with LR, and the lack of local control associated with pathogenic mutations appears to lead to higher rates of death.

NFE2L2 Target Gene Expression Does Not Predict LR after RT

Because prior studies have suggested an association of the expression of NFE2L2 target genes and resistance to radiation (25), we next explored whether NFE2L2 target gene expression is also associated with LR after RT. To do so we performed RNA sequencing (RNA-seq) on formalin-fixed, paraffin-embedded biopsy samples from 41 (42.3%) patients in the SABR and CRT cohorts who had sufficient tissue remaining after DNA sequencing. In order to focus on gene expression of tumor cells, we used CIBERSORTx digital cytometry to infer tumor cell–specific gene-expression profiles and scored samples for the presence of a previously defined NFE2L2 target gene signature (Fig. 3F; refs. 26, 27). We observed significantly higher expression of NFE2L2 target genes in tumors harboring pathogenic *KEAP1/NFE2L2* versus wild-type/passenger mutations ($P = 0.01$; Fig. 3G). Expression of NFE2L2 targets was not significantly associated with LR by Cox regression (HR = 2.33; 95% CI, 0.06–84.30; $P = 0.64$) and did not stratify risk of LR in competing risk analysis ($P = 0.93$; Fig. 3H). Similarly, there was no difference in OS in the TCGA radiation cohort ($P = 0.48$; Fig. 3I). Taken together, these results suggest that although *KEAP1/NFE2L2* mutation status is predictive of clinical response to radiation, expression of NFE2L2 target genes is not.

Glutaminase Inhibition Selectively Radiosensitizes *KEAP1*-Mutant Cells

Finally, we wished to identify a potential approach for radiosensitizing *KEAP1/NFE2L2*-mutant tumors. Recent work

Figure 2. Functional analysis of *KEAP1/NFE2L2* mutations found in the RT cohorts identifies pathogenic and passenger mutations. **A,** Strategy for assessing *KEAP1/NFE2L2* mutation functional classification using isogenic H1299 knockout cell lines generated by CRISPR/Cas9 (images were produced and modified from Servier Medical Art; see Acknowledgments). RNA-seq, RNA sequencing. **B,** Western blot analysis for KEAP1, NFE2L2, and NFE2L2 target proteins in parental and *KEAP1*^{NULL} H1299 cells. **C,** Clonogenic survival of parental and *KEAP1*^{NULL} H1299 cells after 10 Gy of ionizing radiation ($n = 5$; **, $P < 0.001$). **D,** DNA damage assessment by γH2AX foci immunofluoresence analysis 5 minutes after exposure to 2 Gy of ionizing radiation (IR) in parental and *KEAP1*^{NULL} H1299 cells ($n = 4$; ***, $P < 0.0001$; ns, not significant). **E,** Clonogenic survival of parental and *KEAP1*^{NULL} H1299 cells in the presence or absence of BSO (100 nmol/L) and/or NAC (100 mmol/L) treated with or without 4 Gy of ionizing radiation ($n = 4$; Student *t* test, *, $P < 0.01$). **F,** Expression of the NFE2L2 target gene *HMOX1* in *KEAP1*^{NULL} cells by qRT-PCR after transfection of empty plasmid, plasmid containing wild-type (WT) *KEAP1*, or plasmids containing *KEAP1* constructs with mutations observed in the CRT and SABR cohorts ($n = 4$; *, $P < 0.01$). **G,** Clonogenic survival of *KEAP1*^{NULL} cells transfected with plasmids containing wild-type or mutant *KEAP1* constructs 24 hours before exposure to 5 Gy of ionizing radiation. Experiments were performed in groups, with empty vector and wild-type (WT) controls in each group ($n = 3$–4; *, $P < 0.01$; **, $P < 0.001$ compared with "empty" by Student *t* test). **H,** Expression of NFE2L2 target genes in *NFE2L2*^{NULL} or *KEAP1*^{NULL} cells by qRT-PCR after transfection of plasmids containing wild-type or mutant *NFE2L2* ($n = 4$; *, $P < 0.01$). **I,** Clonogenic survival of *NFE2L2*^{NULL} cells transfected with plasmids containing wild-type or mutant *NFE2L2* constructs 24 hours before exposure to 3 Gy of ionizing radiation ($n = 3$; **, $P < 0.001$ by Student *t* test). **J,** Summary of functional assay results and mutation classification for each *KEAP1* and *NFE2L2* mutation found in the CRT and SABR cohorts. NA, not applicable.

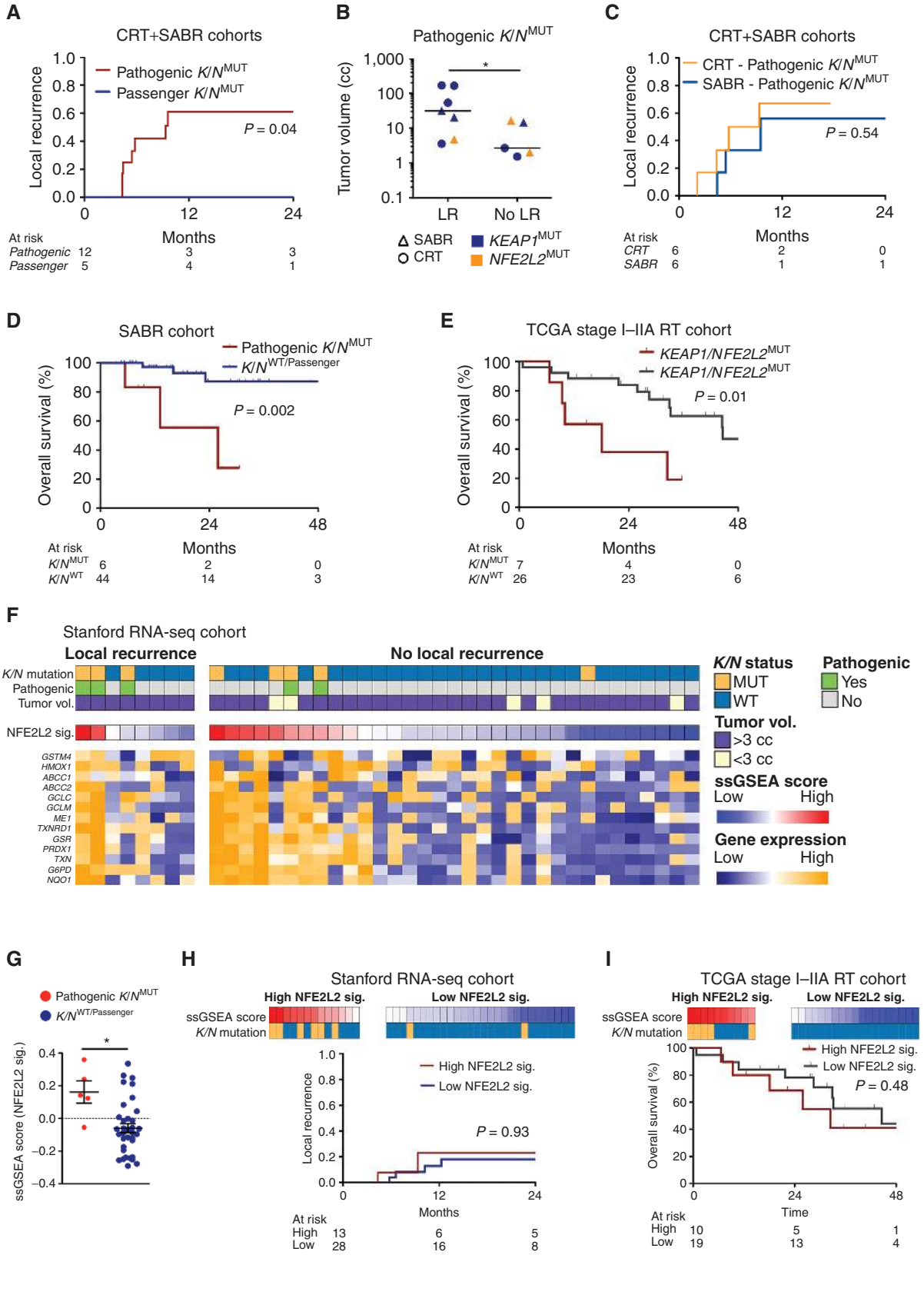

has demonstrated that *KEAP1* loss promotes dependence on glutamine metabolism and sensitivity to glutaminase inhibition (28, 29). Because glutamine metabolism includes production of GSH, a critical antioxidant that has been linked to resistance to ionizing radiation, we hypothesized that glutaminase inhibition can preferentially radiosensitize *KEAP1/NFE2L2*-mutant cells (Fig. 4A). To test this hypothesis, we first examined expression of the glutamine transporter alanine–serine–cysteine transporter 2 (ASCT2) in our isogenic cell lines and observed increased expression in *KEAP1*^{NULL} and decreased expression in *NFE2L2*^{NULL} H1299 cells (Fig. 4B and Supplementary Fig. S8A). Similarly, siRNA-mediated knockdown of *NFE2L2* in H1975 NSCLC cells (*KEAP1/NFE2L2* wild-type) resulted in decreased ASCT2 expression. Furthermore, RNA-seq analysis of both *KEAP1*^{NULL} compared with *KEAP1*^{WT} H1299 cells and tumor biopsy specimens from patients with pathogenic *KEAP1/NFE2L2* mutations ($n = 5$) compared with patients without ($n = 36$) revealed significant overexpression of genes involved in glutamine metabolism (Fig. 4C and D). Thus, both *KEAP1*-mutant human tumors and our *KEAP1*^{NULL} cell lines display upregulation of genes involved in glutamine metabolism.

To explore if targeting of glutamine metabolism can preferentially radiosensitize *KEAP1/NFE2L2*-mutant cells, we tested the combination of RT and the small-molecule glutaminase inhibitor CB-839, which is currently in phase I/II clinical trials, in NSCLC cell lines of differing genetic backgrounds (Fig. 4E). Although *KEAP1*^{NULL} and *KEAP1*^{WT} H1299, H1437, and A549 cells displayed minimal sensitivity to CB-839 doses in the range of 10 to 100 nmol/L, the combination of ionizing radiation and CB-839 preferentially killed *KEAP1*^{NULL} cells (Fig. 4F–I). The sensitization effect was substantial, with a dose-modifying factor for CB-839 in H1299 *KEAP1*^{NULL} cells of 3.4 (at 63% survival; Fig. 4F). Importantly, we observed this effect starting with parental cell lines that were either *KEAP1* wild-type (H1299 and H1437) or mutant (A549). For the latter, treating A549 cells with 100 nmol/L CB-839 did not have a dramatic effect on cell survival but sensitized cells to ionizing radiation (Fig. 4I and Supplementary Fig. S8B and S8C). However, expression of wild-type *KEAP1* in A549 cells increased radiation sensitivity and abolished the sensitizing effect of CB-839. Thus, CB-839 preferentially radiosensitizes *KEAP1*^{NULL} cells.

Lastly, we investigated the mechanism by which CB-839 preferentially radiosensitizes *KEAP1*^{NULL} cells and hypothesized that glutaminase inhibition counteracts the enhanced free radical defenses caused by loss of *KEAP1*. We first examined the effects of CB-839 and ionizing radiation on intracellular reactive oxygen species (ROS) levels. *KEAP1*^{NULL} H1299 cells displayed significantly lower baseline levels of ROS than their wild-type counterparts. However, unlike in *KEAP1*^{WT} H1299 cells, the combination of CB-839 and radiation significantly increased ROS levels in *KEAP1*^{NULL} H1299 cells compared with radiation alone (Fig. 4J). Additionally, CB-839 treatment decreased GSH to glutathione disulfide (GSSG) ratios significantly more in *KEAP1*^{NULL} than in *KEAP1*^{WT} H1299 cells (Fig. 4K). This suggests that CB-839 leads to decreased free radical scavenging capacity in *KEAP1*^{NULL} cells. We next tested if exogenous addition of a free radical scavenger can rescue *KEAP1*^{NULL} cells from CB-839–mediated radiosensitization. Treatment of H1299 *KEAP1*^{NULL} cells with the ROS scavenger NAC did not significantly affect cell survival by itself or when combined with either 2 Gy or CB-839 alone. However, NAC significantly rescued the enhanced cell killing caused by the combination of 2 Gy and CB-839 (Fig. 4L), suggesting that CB-839 radiosensitization is mediated by depletion of free radical scavengers. Finally, we reasoned that if this mechanism is correct, CB-839 should increase the amount of DNA damage induced by ionizing radiation. To test this, we measured DNA double-strand breaks via γH2AX before and after ionizing radiation in the presence or absence of CB-839. Irradiation with 2 Gy induced approximately 2-fold higher levels of γH2AX in *KEAP1*^{WT} compared with *KEAP1*^{NULL} cells (Fig. 4M). Strikingly, 24-hour pretreatment with CB-839 resulted in elevation of γH2AX in *KEAP1*^{NULL} but not *KEAP1*^{WT} cells. These data indicate that CB-839 preferentially radiosensitizes *KEAP1*^{NULL} cells by decreasing free radical scavenging capacity and therefore increasing the amount of DNA damage caused by the indirect effect of ionizing radiation.

DISCUSSION

In summary, in this study we demonstrate that *KEAP1/NFE2L2* mutations are a common cause of LR in patients with localized NSCLC treated with RT but not surgery. These mutations are therefore clinically relevant predictive biomarkers of radioresistance. Using functional analyses including radiation clonogenic assays, we found that 60% of *KEAP1* mutations and all *NFE2L2* mutations in our cohort were pathogenic, and that pathogenic mutations were associated with a ~60% rate of LR after RT but not surgery. Additionally, we show that the glutaminase inhibitor CB-839 preferentially sensitizes *KEAP1*-mutant NSCLC cells to RT.

Of the recurrent mutations found in our cohort, only *KEAP1/NFE2L2* mutations were statistically significantly

Figure 3. Pathogenic *KEAP1/NFE2L2* mutations but not passenger mutations or expression analysis predict LR after RT. **A,** Incidence of LR after CRT or SABR in patients with *KEAP1/NFE2L2* mutations stratified by functional classification. **B,** Tumor volumes for patients with pathogenic *KEAP1/NFE2L2* mutations (K/N^{MUT}). For patients who did not develop LR, the volume of the largest lesion is shown (*, $P = 0.03$). **C,** Incidence of LR in patients with pathogenic *KEAP1/NFE2L2* mutations stratified by RT type. **D,** OS of patients in the SABR cohort stratified by the presence or absence of pathogenic *KEAP1/NFE2L2* mutations. **E,** OS of stage I–II patients from the TCGA lung adenocarcinoma and squamous cell cohorts who were treated with RT and not surgery, stratified by the presence or absence of *KEAP1/NFE2L2* mutations. **F,** RNA-seq analysis of tumor cells from formalin-fixed, paraffin-embedded tumor biopsies of patients in the CRT and SABR cohorts ($n = 41$). CIBERSORTx was used to deconvolve tumor cell expression (26). The heat map depicts single-sample gene set enrichment analysis (ssGSEA) scores of a previously defined NFE2L2 target gene-expression signature (NFE2L2 sig.) and expression of the individual signature genes (27). **G,** NFE2L2 target gene ssGSEA scores in tumor biopsies from patients in the CRT and SABR cohorts stratified by the presence or absence of pathogenic *KEAP1/NFE2L2* mutations. *, $P = 0.01$. **H,** Incidence of LR after CRT or SABR stratified by ssGSEA scores for NFE2L2 signature. Legend is the same as in **F**. Stratification threshold was obtained by choosing the highest significance value by log-rank for LR based on 1,000 resampling iterations. **I,** OS of patients from the TCGA lung adenocarcinoma and squamous cell cohorts who were treated with RT and not surgery, stratified by ssGSEA scores for NFE2L2 signature. The optimal cutoff point identified in **H** was used.

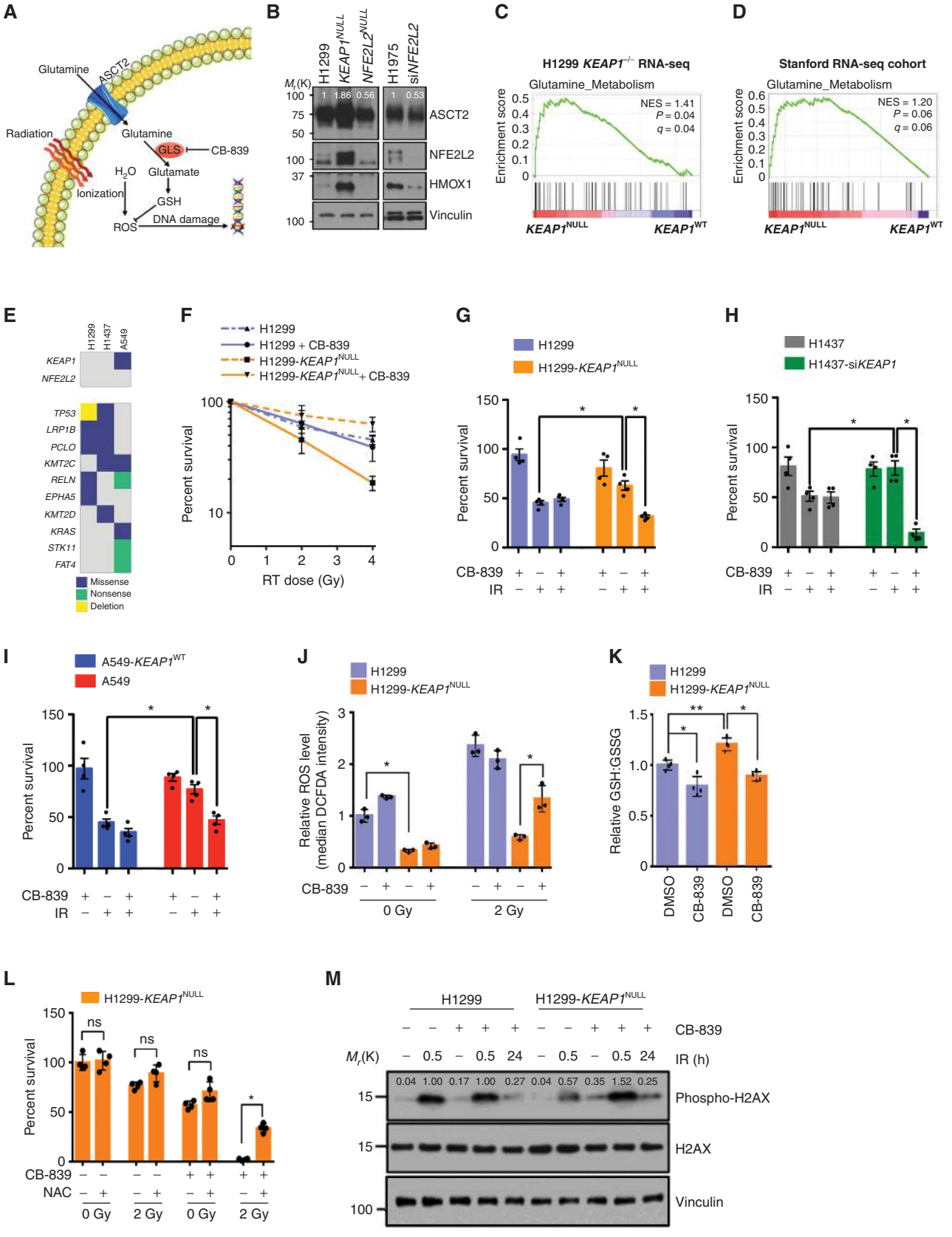

associated with LR. This finding both validates and extends our prior analysis of a smaller, independent cohort in which we examined *KEAP1/NFE2L2* mutations and found that these were associated with LR after RT (17). Overall, nearly half of all LRs occurred in tumors with these mutations, suggesting that *KEAP1/NFE2L2* mutations are a dominant biological driver of clinical radioresistance in localized NSCLC. Comutations in other frequently mutated genes such as lung cancer drivers were not associated with LR. Additionally, unlike other prior studies, we did not observe an association of *KRAS* and/or *TP53* mutations with LR (12, 13). One potential explanation for this discrepancy is that *KEAP1* mutations often co-occur with both *KRAS* and *TP53* mutations, and *KEAP1/NFE2L2* genotyping was not performed in the prior studies. In an exploratory analysis, we also examined if *STK11* mutations were associated with LR after RT because these have been implicated in treatment resistance to other therapies (28, 30, 31). However, only one of five *STK11*-mutant tumors in our RT cohorts developed LR, and this was not statistically significantly different from wild-type tumors (Supplementary Fig. S9; P = ns). Of note, this tumor also carried a pathogenic *KEAP1* mutation, suggesting that it was the likely cause of LR. However, we cannot rule out that there may be additional mutations beyond *KEAP1/NFE2L2* that are associated with radioresistance and that our study was underpowered to detect. That said, our findings suggest that discovering such mutations will require very large cohorts and that other mutations are unlikely to match *KEAP1/NFE2L2* mutations in recurrence frequency and/or effect size.

We were surprised to find high rates of LR in patients with *KEAP1/NFE2L2* mutations who were treated with SABR, which delivers significantly higher doses of ionizing radiation to tumors than conventionally fractionated RT. We found no statistically significant difference in the 2-year LR rate after CRT (67%) and SABR (56%), suggesting dose escalation alone is not sufficient to significantly improve local control in these patients. However, it is possible that our study was underpowered to detect a modest benefit of dose escalation. Indeed, the fact that smaller tumors with *KEAP1/NFE2L2* mutations had better local control suggests dose escalation may be useful in some settings. Notably, our results and prior studies have shown that increasing rates of LR in patients with stage I–II NSCLC are associated with worse OS, highlighting the need to achieve better local tumor control in this setting (2, 32).

By expressing mutant alleles in knockout cell lines, we found that ~40% of *KEAP1* mutations in our RT cohorts have neutral effects on KEAP1 function and are therefore likely passenger mutations. This is somewhat higher than in a prior study in which 4/18 (22%) *KEAP1* mutations found in a lung squamous cell carcinoma cohort were determined to have neutral effects on KEAP1 activity (33). We compared four functional assays for KEAP1/NFE2L2 pathway activity, including NFE2L2 target mRNA expression, NFE2L2 target protein expression, resistance to hydrogen peroxide, and resistance to ionizing radiation. Variants demonstrated similar patterns in all four assays and behaved either as loss of function or neutral alleles. Notably, two of the mutations (R204P and R320Q) found in our SABR cohort had also been included in prior studies and were classified as hypomorphic variants (33, 34). One of these (R204P) behaved like a loss-of-function allele in our assays and was found in a patient who developed LR, while the other (R320Q) behaved like a passenger mutation and was found in a patient who did not have LR. Thus, functional classification of *KEAP1* variants may be context dependent, and the knockout cell line system we established faithfully recapitulates radiation resistance phenotypes observed clinically.

Because pathogenic *KEAP1/NFE2L2* mutations result in overexpression of NFE2L2 target genes, we tested whether analysis of gene expression could also identify tumors at highest risk of LR. Interestingly, we observed that whereas tumors with *KEAP1/NFE2L2* mutations did tend to overexpress NFE2L2 target genes, a significant subset of wild-type tumors also displayed overexpression. Unlike genotyping for *KEAP1/NFE2L2* mutations, high expression of NFE2L2 target genes did not stratify LR or OS. One potential explanation for this observation is that stress induced by ischemia and/or tissue handling might affect expression of NFE2L2 target genes, as has been demonstrated for *NQO1* (35). Separately, NFE2L1 (also called NRF1) shares many downstream target genes with NFE2L2, and it is possible that *KEAP1/NFE2L2* wild-type tumors with high expression of NFE2L2 target genes may have enhanced NFE2L1 activity (36). Although more work is needed in this area, our results

Figure 4. Glutaminase inhibition preferentially radiosensitizes *KEAP1*-mutant lung cancer cells. **A,** Schematic depicting potential interaction between glutaminase inhibition and ionizing radiation in *KEAP1*-mutant cells (images were produced and modified from Servier Medical Art; see Acknowledgments). **B,** Western blot analysis for ASCT2, NFE2L2, and HMOX1. Left, parental, *KEAP1*^{NULL}, and *NFE2L2*^{NULL} H1299 cells. Right, transient siRNA knockdown of *NFE2L2* in H1975 NSCLC cells (wild-type for *KEAP1* and *NFE2L2*). **C,** Gene set enrichment analysis of a previously defined glutamine metabolism signature using RNA-seq data from parental and *KEAP1*^{NULL} H1299 cells. **D,** As in **C** but using RNA-seq data from the tumor biopsies of patients in the CRT and SABR cohorts, comparing samples with and without pathogenic *KEAP1* mutations. **E,** Oncoprint of genes recurrently mutated in NSCLC (24) in the three cell lines used for the experiments with CB-839. **F,** Clonogenic survival of parental and *KEAP1*^{NULL} H1299 cells in the presence or absence of CB-839 (100 nmol/L; 24-hour pretreatment) and 4 Gy of ionizing radiation ($n = 4$). Results were normalized against untreated cells. **G,** Clonogenic survival of *KEAP1*^{NULL} and parental H1299 cells (*KEAP1* wild-type) in the presence or absence of CB-839 (100 nmol/L; 24-hour pretreatment) and 4 Gy of ionizing radiation ($n = 4$; *, $P < 0.01$). **H,** Clonogenic survival of H1437 cells (*KEAP1* wild-type) with and without siRNA knockdown of *KEAP1* in the presence or absence of 2 Gy and 500 nmol/L CB-839 ($n = 4$; *, $P < 0.01$). **I,** Clonogenic survival of parental and *KEAP1*-transfected A549 cells (KEAP1 mutant) in the presence or absence of CB-839 (0.1 nmol/L; 24-hour pretreatment) and 2 Gy of ionizing radiation ($n = 4$; *, $P < 0.01$; **, $P < 0.001$). Results for **F–I** were normalized to untreated cells. **J,** Intracellular ROS levels measured by DCFDA intensity via FACS in parental and *KEAP1*^{NULL} H1299 cells in the presence or absence of CB-839 (100 nmol/L; 24-hour pretreatment) and 2 Gy of ionizing radiation ($n = 4$; *, $P < 0.01$). **K,** GSH:GSSG ratio in parental and *KEAP1*^{NULL} H1299 cells in the presence or absence of CB-839 (1 μmol/L; 24-hour pretreatment; $n = 4$; *, $P < 0.05$; **, $P < 0.01$). **L,** Clonogenic survival of *KEAP1*^{NULL} H1299 cells treated with or without 2 Gy of ionizing radiation and/or 100 nmol/L CB-839 in the presence or absence of NAC (1 mmol/L; $n = 4$; *, $P < 0.01$; ns, not significant). **M,** Western blot analysis for γH2AX in parental and *KEAP1*^{NULL} H1299 cells in the presence or absence of CB-839 (100 nmol/L) treated with or without 2 Gy IR.

suggest that tumor genotyping for *KEAP1/NFE2L2* mutations is the most reliable method for identifying radioresistant NSCLCs.

A key implication of our findings is the need to develop strategies for overcoming *KEAP1/NFE2L2*-mediated radioresistance. Our analysis of DNA double-strand breaks after ionizing radiation suggests that *KEAP1* loss leads to radioprotection by decreasing DNA damage via enhanced free radical scavenging. Consistent with this hypothesis, *KEAP1*^{NULL} cells display lower ROS levels and higher levels of GSH, a key intracellular antioxidant that has previously been implicated in contributing to radioresistance (29, 37). Furthermore, depletion of GSH via BSO radiosensitized *KEAP1*^{NULL} cells to levels similar to those in *KEAP1*^{WT} cells, suggesting that the mechanism of radioresistance is largely mediated by increased GSH production. We therefore tested the hypothesis that glutaminase inhibition, which decreases GSH production, preferentially radiosensitizes *KEAP1*-mutant cells. Our interest in glutaminase was in part based on prior observations that *KEAP1*-mutant NSCLC is dependent on glutamine metabolism (28, 29) and that inhibition of glutamine metabolism may be of therapeutic benefit in NSCLC (38–42). Strikingly, we found that low doses of the glutaminase inhibitor CB-839 (0.1–500 nmol/L), which is currently in clinical trials in other contexts, can preferentially radiosensitize *KEAP1*-mutant but not isogenic wild-type cells in three different NSCLC cell line models. CB-839 sensitized *KEAP1*^{NULL} cells to similar levels as *KEAP1*^{WT} cells, suggesting that this approach could improve local control of *KEAP1*-mutant tumors to similar levels as that of wild-type tumors. Additionally, we expect that the ~2-fold increase in cell killing we observed in *KEAP1*^{NULL} cells treated with CB-839 after a single dose of RT would be compounded over a multifraction course, leading to potentially dramatic increases in total cell killing.

Mechanistic analyses demonstrated that CB-839 pretreatment leads to depletion of free radical scavengers and increased DNA damage via the indirect effect of radiation. Although our analyses were focused on *in vitro* experiments, a recent study by another group demonstrated that CB-839 can radiosensitize *KEAP1*-mutant cells *in vivo*. Specifically, Boysen and colleagues treated H460 NSCLC xenografts grown in nude mice with CB-839, 12 to 18 Gy of radiation, or both (43). The combination of CB-839 plus radiation significantly delayed tumor growth compared with radiation alone. Although not mentioned by Boysen and colleagues, H460 cells carry the pathogenic *KEAP1* D236H mutation (44). Thus, CB-839 radiosensitization appears to be a promising approach for overcoming *KEAP1/NFE2L2* mutation-mediated radioresistance.

We have now validated the association of *KEAP1/NFE2L2* mutations with inferior outcomes after RT in four independent cohorts of patients with NSCLC (one from our prior report and three in the current report; ref. 17). Our findings therefore have potential implications for the clinical management of patients with *KEAP1/NFE2L2*-mutant NSCLC. For medically operable patients with node-negative disease who are candidates for surgery or SABR, surgery may be preferable because it does not appear to be associated with increased rates of LR. For medically operable patients with lymph node–positive NSCLC, the presence of *KEAP1/NFE2L2* mutations is more complicated because these patients usually receive RT and/or surgery plus chemotherapy, and these mutations have also been linked to chemoresistance (45, 46). Such patients may therefore be ideal candidates for trimodality therapy consisting of surgery, RT, and chemotherapy, because surgical debulking should increase the chance that RT and chemotherapy can eliminate any clonogens remaining after surgery. Our finding that local control of *KEAP1/NFE2L2*-mutant tumors appears to be better in smaller tumors with fewer clonogens supports this idea. For medically inoperable early-stage patients, a radiosensitization strategy such as treatment with CB-839 might be beneficial. Lastly, based on several randomized phase II trials demonstrating survival benefits, use of SABR in patients with NSCLC with oligometastatic disease appears to be a promising approach for improving survival (47–49). Our findings suggest that patients with oligometastatic NSCLC with *KEAP1/NFE2L2*-mutant tumors will likely have inferior local control if treated with SABR alone and therefore might benefit from radiosensitization with CB-839. Because RT is frequently delivered with systemic therapies, future studies will also need to ensure that CB-839 does not increase toxicity in combination therapy settings.

Limitations of our study include its retrospective nature and that all patients were treated at a single institution. Thus, although we have validated the association of *KEAP1/NFE2L2* mutations with LR after RT in multiple cohorts, it would be useful to repeat these analyses in cohorts from other institutions in the future. Additionally, LR was relatively uncommon and thus forced us to limit our analyses to mutations with sufficient recurrence frequency. Furthermore, because our cohort was genotyped using a targeted assay, it is possible that mutations in genomic regions that were not covered might also be associated with LR. Lastly, there were significant differences in patient characteristics between the SABR and surgery cohorts that reflect the types of patients who receive each therapy and that could have confounded the comparison of the two groups. However, the fact that tumor size/stage, which to our knowledge is the only consistently reported parameter associated with LR after either treatment, did not differ between the two cohorts decreases this risk (9, 50).

In conclusion, in a large cohort of patients with localized NSCLC treated with definitive radiation or surgery, we have demonstrated that *KEAP1/NFE2L2* mutations are strongly predictive of LR after RT but not surgery. Furthermore, functional classification of *KEAP1/NFE2L2* mutations revealed that only pathogenic mutations that lead to radioresistance *in vitro* were associated with LR clinically. Finally, glutaminase inhibition may offer a strategy for a precision radiation oncology approach for radiosensitizing *KEAP1/NFE2L2*-mutant tumors.

METHODS

Study Design and Patient Selection

Using prospective registries of patients with NSCLC treated with RT (2009–2018) or surgery (2015–2018) at Stanford University School of Medicine, we performed a retrospective study with institutional review board approval of all consecutive patients with American Joint Committee on Cancer (AJCC) 8th edition stage IA1–IIIC NSCLC who

had clinical next-generation sequencing (NGS) performed on tumor tissue with baseline characteristics shown in Supplementary Table S1. We excluded patients who were included in our previously published cohort of RT-treated patients with *KEAP1/NFE2L2* tumor genotyping in order to ensure analysis of a completely independent cohort (17).

Our primary goal was to evaluate the association between somatic tumor mutations and LR in patients with localized NSCLC receiving CRT or SABR. Given that these cohorts totaled 97 patients, we calculated that in order to achieve 80% power to detect an absolute difference in LR rate of ≥15% at 2 years (alpha = 0.05), a gene would need to be mutated in ≥6 patients. We therefore only considered genes above this recurrence threshold.

Patient Cohorts

The CRT cohort (Supplementary Table S4) consisted of patients with stage IIB–IIIC NSCLC, and the SABR cohort (Supplementary Table S5) consisted of patients with stage IA1–IIB NSCLC. We have previously reported our RT treatment protocols (10, 51). Follow-up post-RT consisted of CT and/or PET-CT imaging at 3-month intervals during the first 2 years, 6-month intervals during the next 2 years, and yearly thereafter.

Patients in the surgery cohort had stage IA1–IIB NSCLC and underwent surgery without neoadjuvant or adjuvant chemotherapy. Patients underwent wedge resection, segmentectomy, or lobectomy with or without selective ipsilateral hilar and mediastinal nodal dissections. Follow-up visits occurred at 6-month intervals, with CT performed at each visit.

LR was defined as tumor regrowth within the RT planning target volume (PTV) for the RT cohorts and recurrence at the staple line or bronchial stump for the surgery cohort. LR was scored using pathologic confirmation or by radiologic changes consistent with tumor regrowth. Radiologic criteria for LR were: (i) interval increase in size of a mass-like lesion on CT and/or (ii) interval increase in FDG uptake in a focal pattern on PET. Whenever possible, we confirmed radiologic findings on serial imaging in the context of overall disease progression. Radiologic scoring of LR was done by a single investigator (M.S. Binkley) blinded to the tumor-genotyping results.

MTV Analysis

We used the "PET Edge" tool in MIMvista software, a gradient-based algorithm, to delineate the MTV of individually distinct lesions on attenuation-corrected PET scans as previously described (10, 52). For lesion-specific MTV analyses in CRT patients, the MTV of the lesion that recurred was used in patients with LR and the MTV of the largest targeted lesion was used in patients who did not develop LR.

Tumor Genotyping

Tumor genotyping was performed in the Stanford Molecular Pathology CLIA laboratory on formalin-fixed, paraffin-embedded tumor tissue via a laboratory-developed test NGS assay called the "STanford Actionable Mutation Panel" (STAMP), as previously described (20). Two versions of the assay were used during the years of the study covering 130 or 198 genes (both including all exons of *KEAP1, NFE2L2, TP53*, and *KRAS*). Mutation calls were extracted from clinical genotyping reports. Lung cancer driver genes were defined as *EGFR, KRAS, NRAS, PIK3CA, HER2, BRAF, MET, ALK, ROS1, RET*, and *NTRK1/2/3*. Copy-number alteration analysis was performed as previously described considering both on-target and off-target reads (53). Activating mutations in *KRAS* (codons 12 and 13) and *EGFR* (exons 18–21; ref. 54) were considered pathogenic. All other mutations with Combined Annotation Dependent Deletion (CADD) PHRED scores ≥20 and with a population frequency of <1% in the genome aggregation database (Broad Institute, v3; ref. 55) were considered pathogenic. Mutations in *NFE2L2* were considered pathogenic if they were located in the Neh2 domain (amino acids 16–86) that interacts with *KEAP1* and had CADD PHRED scores ≥20. Final tumor genotyping used for analysis is summarized in Supplementary Table S6.

RNA-seq

Isolation of RNA from formalin-fixed, paraffin-embedded tumor tissue was performed for cases with sufficient tissue remaining using the RNAstorm kits (CELLDATA) with DNAse digestion (Qiagen) and subsequent purification with RNA Clean and Concentrator kits (Zymo Research). Sequencing libraries were prepared using the SMARTer Stranded total RNA-seq Kit v2 (Takara Bio USA, Inc.) and sequenced on the Illumina HiSeq4000 platform with paired-end 150-bp reads and 14 to 16 samples per lane. Gene-expression levels were quantified using Salmon (v0.8.2) under quasi-mapping mode to Gencode version 27 (56). Transcript per million (TPM; Supplementary Table S7) values were used as input for CIBERSORTx digital cytometry, allowing for inference of tumor cell–specific gene-expression profiles using a reference transcriptome of flow-sorted malignant, endothelial, immune, and fibroblast cell expression profiles (26, 57). Differential gene-expression analysis and normalization were conducted with the package "DESeq2." Single and bulk sample gene set enrichment and gene set variation analyses were performed with GSVA.

Cell Culture, Plasmids, and Nucleic Acid Delivery

H1299 and A549 cells were purchased from the ATCC. The H1299 cell line was cultured in RPMI-1640 supplemented with 10% fetal bovine serum (FBS), and A549 cells were maintained in DMEM with 10% FBS. All cell lines were tested for *Mycoplasma* and were negative using PlasmoTest (Invivogen). *KEAP1* or *NFE2L2* plasmids were purchased from Addgene (#87545 for *KEAP1* and #21555 for *NFE2L2*), and the *KEAP1* or *NFE2L2* cDNA was subcloned into the pcDNA4-V5-His vector (Invitrogene, #V861-20). Site-directed mutagenesis was performed to generate *KEAP1* and *NFE2L2* alleles bearing mutations identified in patients from the RT cohorts using QuickChange II site-Directed Mutagenesis Kit (Agilent, #200524) and confirmed with Sanger sequencing. Transient expression of these constructs as well as siRNAs was performed using Lipofectamine 3000 as per the manufacturer's protocol (Invitrogen). Cell viability was measured using the CellTiter-Glo Luminescent Cell Viability Assay kit (Promega, #G7572) or clonogenic assays. For the latter, cells were cultured for 1 to 2 weeks, and colonies greater than 50 densely packed cells were counted using crystal violet staining. Quantitation was performed using ImageJ software as previously described (58). The survival fraction was calculated based on the plating efficiency, number of colonies, and number of seeded cells [SF = colonies counted/(cells seeded × plating efficiency)]. For experiments involving mutant alleles, cells were transfected with plasmids ≥72 hours prior to treatment with ionizing radiation and/or CB-839.

Antibodies

Anti-ASCT2 (#8057), anti-GAPDH (#5174), anti-HMOX1 (#5061), anti-KEAP1 (#8047, used to detect endogenous KEAP1 protein), anti-NQO1 (#3187), anti-P62 (#88588), anti–phospho-Histone H2AX (#9718), anti-ubiquitin (#3936), and anti-Vinculin (#13901) antibodies were purchased from Cell Signaling Technology and used at 1:1,000 dilution for Western blot analysis and 1:100 dilution for immunoprecipitation and immunofluorescence analysis. Polyclonal anti-KEAP1 antibody (#10503), used to detect KEAP1-mutant proteins because some lacked binding site for the monoclonal anti-KEAP1 antibody, was purchased from Protein-Tech and used at 1:1,000 dilution for Western blot analysis. Anti-V5 antibody (#MA5-15253) was purchased from Invitrogen and used at 1:5,000 dilution for Western blot analysis. Anti-flag M2 antibody (F3165) was purchased from Sigma-Aldrich and

used at 1:100 dilution for immunoprecipitation analysis. All antibodies were monoclonal except anti-HMOX1 and anti-KEAP1 (#10503).

Isogenic Cell Line Generation

The sgRNAs for *KEAP1* or *NFE2L2* gene were designed using the Genetic Perturbation Portal (Broad Institute). To generate knockout cell lines, sgRNAs and Cas9 protein (Integrated DNA Technologies, Inc., # 1081058) complexes were nucleofected into H1299 cell. After 48 hours, single cells were sorted into 96-well plates. After 2 to 3 weeks, colonies were harvested and *KEAP1* or *NFE2L2* knockout was confirmed by qRT-PCR, Western blot, and gDNA sequencing analyses. In order to prevent exogenous overexpression of wild-type NFE2L2 from overcoming the capacity of endogenous KEAP1 to degrade it, we cotransfected a wild-type KEAP1–containing plasmid with plasmids containing NFE2L2 constructs into NFE2L2^{NULL} H1299 cells (Fig. 2I and J; Supplementary Fig. S6C–S6E). To generate A549-*KEAP1* cells, *KEAP1* cDNA was subcloned into the pCDH lentiviral vector (System Bioscience). A549 cells were then transduced with the virus, followed by selection using puromycin (1 μg/mL) for 7 days. Stable cell line generation was confirmed by qRT-PCR and Western blot analyses. The sequences of all sgRNAs and siRNAs are listed in Supplementary Fig. S4.

Classification of KEAP1 *and* NFE2L2 *Mutations*

KEAP1 mutations were scored as being neutral (i.e., passengers) in the various assays if they displayed: (i) decreased *HMOX1* mRNA expression compared with *KEAP1*^{NULL} cells transfected with empty vector ($P < 0.05$), (ii) increased H_2O_2 sensitivity in CellTiter-Glo assays compared with *KEAP1*^{NULL} H1299 cells transfected with empty vector ($P < 0.05$), (iii) decreased NFE2L2 target gene protein expression compared with *KEAP1*^{WT} H1299 cells by visual scoring, and (iv) increased radiation sensitivity in clonogenic assays compared with *KEAP1*^{NULL} H1299 cells transfected with empty vector ($P < 0.05$). *KEAP1* mutations not meeting these criteria were scored as loss-of-function (i.e., pathogenic). *NFE2L2* mutations were scored as being gain-of-function (i.e., pathogenic) in the various assays if they displayed: (i) increased *HMOX1* mRNA expression compared with *NFE2L2*^{NULL} cells transfected with *NFE2L2*^{WT} vector ($P < 0.05$), (ii) increased NFE2L2 target gene protein expression compared with *NFE2L2*^{NULL} cells transfected with *NFE2L2*^{WT} vector by visual scoring, and (iii) increased radiation resistance in clonogenic assays compared with *NFE2L2*^{NULL} cells transfected with *NFE2L2*^{WT} vector ($P < 0.05$).

Cell Cytotoxicity Assay

A549, H1299, and their isogenic cell lines (1.0×10^3 cells) were subcultured into 96-well plates. After 24 hours, the cells were treated with CB-839 for 72 hours or hydrogen peroxide for 24 hours as indicated concentration in the figure legend; the cells were subsequently subject to CellTiter-Glo Luminescent Cell Viability Assay (Promega, #G7572) to determine cell viability as per the manufacturer's protocol.

Measurement for Intracellular ROS and GSH

Cells were preincubated with vehicle, CB-839, or N-acetylcystein (Abcam, #ab143032) for 24 hours and subsequently exposed to ionizing radiation. After an additional 24 hours, cells were stained with 25 μmol/L DCFDA for 45 minutes (Abcam) and evaluated via FACS analysis. The GSH:GSSG ratio was measured using the GSH/GSSG Ratio Detection Assay Kit (Abcam, # ab138881) according to the manufacturer's protocol and quantified using a microplate reader (E_x/E_m = 490/520 nm).

Statistical Analysis

Follow-up was measured using the reverse Kaplan–Meier method from completion of treatment until last thoracic imaging. OS was estimated using the Kaplan–Meier method from the time of completion of RT. All other statistical analyses were conducted with adjustment for the competing risk of death. The cumulative incidence of LR and out-of-field recurrence (recurrence outside of the RT PTV) were measured using the R package "cmprsk." Univariable and multivariable competing risk regressions were conducted with the R package "crrSC." Variables with $P < 0.1$ on UVA were included in MVA. Adjusted Benjamini and Hochberg *P* values were calculated with the R package "stats." Sample size calculation was conducted with the R package "samplesize." For comparison of experimental data, the Mann–Whitney *U* test was used to calculate *P* values unless otherwise specified. All statistical analyses were conducted with R version 3.6 and PRISM version 6. Unless otherwise specified, all error bars represent standard deviation. All *P* values were two-sided and considered significant at $P < 0.05$.

Authors' Disclosures

E.J. Moding reports personal fees from DeciBio (for consultation on the use of biomarkers in cancer) outside the submitted work. J.J. Chabon reports ownership interest in Foresight Diagnostics, paid consultancy from Factorial Diagnostics, and patent filings related to cancer biomarkers. D.M. Kurtz reports personal fees from Roche Molecular Diagnostics (consultancy) and other from Foresight Diagnostics (ownership interest) outside the submitted work, as well as a patent for Methods and Systems for Assessment and Treatment of Cancer pending, a patent for Methods of Treatments Based Upon Updated Probabilities of Clinical Outcome pending, and a patent for Methods of Analyzing Cell Free Nucleic Acids and Applications Thereof pending. N.S. Lui reports grants from Intuitive Surgical Foundation (research grant) outside the submitted work. L.M. Backhus reports personal fees from Johnson and Johnson (speaker) and Guidpoint Consulting (expert consultant) and grants from the Department of Veterans Affairs (HSR&D Grant), and NIH (co-principal investigator on RO1) outside the submitted work. K.J. Ramchandran reports personal fees from Dhristi Inc (advisor), GTX (advisory board meeting), and Varian (advisor) outside the submitted work. S.K. Padda reports grants from Epicentrx (research funding), Bayer (research funding), and Boehringer Ingelheim (research funding) and personal fees from Blueprint (advisory board), G1 Therapeutics (advisory board), CME Solutions (honoraria), Pfizer (advisory board), AstraZeneca (advisory board), PER (honoraria), and 47 Inc. (research funding) outside the submitted work. M. Das reports personal fees from Jazz Pharmaceuticals (consultant), Bristol Myers Squibb (consultant), and AstraZeneca (consultant) and grants from Varian (research funding), AbbVie (research funding), United Therapeutics (research funding), and Novartis (research funding) outside the submitted work. J.W. Neal reports personal fees from Amgen (advisory board), AstraZeneca (advisory board), Calithera Biosciences (advisory board), Eli Lilly and Company (advisory board), Iovance Biotherapeutics (advisory board), Jounce Therapeutics (advisory board), Biomedical Learning Institute (honoraria), CME Matters (honoraria), Medscape (honoraria), MJH CME (honoraria), MLI Peerview (honoraria), Prime Oncology (honoraria), Research to Practice (honoraria), and Rockpointe (honoraria); grants from Adaptimmune (research funding), Boehringer Ingelheim (research funding), GlaxoSmithKline (research funding), Merck (research funding), Nektar Therapeutics (research funding), and Novartis (research funding); and grants and personal fees from Exelixis (advisory board, research funding), Genentech/Roche (advisory board, research funding), and Takeda Pharmaceuticals (advisory board, research funding) outside the submitted work. H.A. Wakelee reports grants from NIH and Ludwig institute for Cancer Research during the conduct of the study, as well as grants and personal fees from Novartis (advisory board, clinical trial support to institution), AstraZeneca (advisory board, clinical trial support to institution), and Xcovery (advisory board, clinical trial support to institution), personal fees from Janssen (advisory board),

Mirati (advisory board), Daiichi Sankyo (advisory board), Helsinn (advisory board), and Blueprint (advisory board), and grants from ACEA Biosciences (clinical trial support to institution), Arrys Therapeutics (clinical trial support to institution), Bristol Myers Squibb (clinical trial support to institution), Celgene (clinical trial support to institution), Clovis (clinical trial support to institution), Genentech/Roche (clinical trial support to institution), Gilead (clinical trial support to institution), Merck (clinical trial support to institution), and Pfizer (clinical trial support to institution) outside the submitted work. A.A. Alizadeh reports grants and personal fees from Celgene; personal fees from Karyopharm, Roche, and Phamacyclics; personal fees and other from Gilead (stock); other from Forty Seven (stock), CiberMed (founder equity), and Foresight Diagnostics (founder equity) outside the submitted work. B.W. Loo reports grants and nonfinancial support from Varian Medical Systems (research funding and technical support) outside the submitted work. M. Diehn reports grants from NIH and Ludwig Institute for Cancer Research during the conduct of the study, as well as personal fees from Roche, AstraZeneca, RefleXion, Novartis, Gritstone, and BioNTech, personal fees and nonfinancial support from Illumina, and grants from Varian Medical Systems outside the submitted work. No disclosures were reported by the other authors.

Authors' Contributions

M.S. Binkley: Conceptualization, data curation, formal analysis, validation, investigation, visualization, methodology, writing–original draft, writing–review and editing. **Y.-J. Jeon:** Conceptualization, data curation, formal analysis, validation, investigation, visualization, methodology, writing–original draft, writing–review and editing. **M. Nesselbush:** Data curation, formal analysis, visualization, writing–original draft, writing–review and editing. **E.J. Moding:** Data curation, investigation, visualization, writing–original draft, writing–review and editing. **B.Y. Nabet:** Data curation, investigation, writing–original draft, writing–review and editing. **D. Almanza:** Data curation, writing–original draft, writing–review and editing. **C. Kunder:** Data curation, investigation, writing–original draft, writing–review and editing. **H. Stehr:** Data curation, investigation, writing–original draft, writing–review and editing. **C.H. Yoo:** Data curation, writing–original draft, writing–review and editing. **S. Rhee:** Data curation, investigation, writing–original draft, writing–review and editing. **M. Xiang:** Data curation, writing–original draft, writing–review and editing. **J.J. Chabon:** Data curation, writing–original draft, writing–review and editing. **E. Hamilton:** Data curation, writing–original draft, writing–review and editing. **D.M. Kurtz:** Data curation, methodology, writing–original draft, writing–review and editing. **L. Gojenola:** Resources, data curation, writing–original draft, writing–review and editing. **S.G. Owen:** Resources, data curation, writing–original draft, writing–review and editing. **R.B. Ko:** Data curation, writing–original draft, writing–review and editing. **J.H. Shin:** Data curation, investigation, writing–original draft, writing–review and editing. **P.G. Maxim:** Writing–original draft, writing–review and editing. **N.S. Lui:** Data curation, writing–original draft, writing–review and editing. **L.M. Backhus:** Data curation, writing–original draft, writing–review and editing. **M.F. Berry:** Data curation, writing–original draft, writing–review and editing. **J.B. Shrager:** Data curation, writing–original draft, writing–review and editing. **K.J. Ramchandran:** Data curation, writing–original draft, writing–review and editing. **S.K. Padda:** Data curation, writing–original draft, writing–review and editing. **M. Das:** Data curation, writing–original draft, writing–review and editing. **J.W. Neal:** Data curation, writing–original draft, writing–review and editing. **H.A. Wakelee:** Data curation, writing–original draft, writing–review and editing. **A.A. Alizadeh:** Data curation, formal analysis, investigation, visualization, methodology, writing–original draft, writing–review and editing. **B.W. Loo Jr:** Resources, data curation, validation, investigation, writing–original draft, writing–review and editing. **M. Diehn:** Conceptualization, resources, data curation, formal analysis, supervision, funding acquisition, validation, investigation, visualization, methodology, writing–original draft, writing–review and editing.

Acknowledgments

This work was supported by grants from the NCI (M. Diehn and A.A. Alizadeh, R01CA188298), the U.S. NIH Director's New Innovator Award Program (M. Diehn, 1-DP2-CA186569), the Ludwig Institute for Cancer Research (M. Diehn and A.A. Alizadeh), the CRK Faculty Scholar Fund (M. Diehn), and in part by PA-14-015, grant number T32 CA 121940, awarded by the Ruth L. Kirschstein National Research Service Award (NRSA), and the National Research Foundation of Korea (NRF) grant funded by the Korean government (Y.-J. Jeon, NRF-2020R1F1A1071579). The schematics for Fig. 1A, Fig. 2A, and Fig. 4A were produced using Servier Medical Art (https://smart.servier.com). Servier Medical Art by Servier is licensed under a Creative Commons Attribution 3.0 Unported License (https://creativecommons.org/licenses/by/3.0/).

The costs of publication of this article were defrayed in part by the payment of page charges. This article must therefore be hereby marked *advertisement* in accordance with 18 U.S.C. Section 1734 solely to indicate this fact.

Received March 8, 2020; revised August 12, 2020; accepted September 16, 2020; published first October 18, 2020.

REFERENCES

1. Siegel RL, Miller KD, Jemal A. Cancer statistics, 2018. CA Cancer J Clin 2018;68:7–30.
2. Machtay M, Paulus R, Moughan J, Komaki R, Bradley JE, Choy H, et al. Defining local-regional control and its importance in locally advanced non-small cell lung carcinoma. J Thorac Oncol 2012;7:716–22.
3. Bradley JD, Paulus R, Komaki R, Masters G, Blumenschein G, Schild S, et al. Standard-dose versus high-dose conformal radiotherapy with concurrent and consolidation carboplatin plus paclitaxel with or without cetuximab for patients with stage IIIA or IIIB non-small-cell lung cancer (RTOG 0617): a randomised, two-by-two factorial phase 3 study. Lancet Oncol 2015;16:187–99.
4. Senthi S, Lagerwaard FJ, Haasbeek CJ, Slotman BJ, Senan S. Patterns of disease recurrence after stereotactic ablative radiotherapy for early stage non-small-cell lung cancer: a retrospective analysis. Lancet Oncol 2012;13:802–9.
5. Ball D, Mai GT, Vinod S, Babington S, Ruben J, Kron T, et al. Stereotactic ablative radiotherapy versus standard radiotherapy in stage 1 non-small-cell lung cancer (TROG 09.02 CHISEL): a phase 3, open-label, randomised controlled trial. Lancet Oncol 2019;20:494–503.
6. Ohri N, Bodner WR, Kabarriti R, Shankar V, Cheng H, Abraham T, et al. Positron emission tomography-adjusted intensity modulated radiation therapy for locally advanced non-small cell lung cancer. Int J Radiat Oncol Biol Phys 2018;102:709–15.
7. van Diessen JN, Chen C, van den Heuvel MM, Belderbos JS, Sonke JJ. Differential analysis of local and regional failure in locally advanced non-small cell lung cancer patients treated with concurrent chemoradiotherapy. Radiother Oncol 2016;118:447–52.
8. Werner-Wasik M, Swann RS, Bradley J, Graham M, Emami B, Purdy J, et al. Increasing tumor volume is predictive of poor overall and progression-free survival: secondary analysis of the Radiation Therapy Oncology Group 93-11 phase I-II radiation dose-escalation study in patients with inoperable non-small-cell lung cancer. Int J Radiat Oncol Biol Phys 2008;70:385–90.
9. Zhao L, Zhou S, Balter P, Shen C, Gomez DR, Welsh JD, et al. Planning target volume D95 and mean dose should be considered for optimal local control for stereotactic ablative radiation therapy. Int J Radiat Oncol Biol Phys 2016;95:1226–35.

10. Gensheimer MF, Hong JC, Chang-Halpenny C, Zhu H, Eclov NCW, To J, et al. Mid-radiotherapy PET/CT for prognostication and detection of early progression in patients with stage III non-small cell lung cancer. Radiother Oncol 2017;125:338–43.
11. Lockney NA, Yang TJ, Barron D, Gelb E, Gelblum DY, Yorke E, et al. PIK3CA mutation is associated with increased local failure in lung stereotactic body radiation therapy (SBRT). Clin Transl Radiat Oncol 2017;7:91–3.
12. Mak RH, Hermann G, Lewis JH, Aerts HJ, Baldini EH, Chen AB, et al. Outcomes by tumor histology and KRAS mutation status after lung stereotactic body radiation therapy for early-stage non-small-cell lung cancer. Clin Lung Cancer 2015;16:24–32.
13. Cassidy RJ, Zhang X, Patel PR, Shelton JW, Escott CE, Sica GL, et al. Next-generation sequencing and clinical outcomes of patients with lung adenocarcinoma treated with stereotactic body radiotherapy. Cancer 2017;123:3681–90.
14. Best SA, Sutherland KD. "Keaping" a lid on lung cancer: the Keap1-Nrf2 pathway. Cell Cycle 2018;17:1696–707.
15. Cancer Genome Atlas Research Network. Comprehensive genomic characterization of squamous cell lung cancers. Nature 2012;489:519–25.
16. Cancer Genome Atlas Research Network. Comprehensive molecular profiling of lung adenocarcinoma. Nature 2014;511:543–50.
17. Jeong Y, Hoang NT, Lovejoy A, Stehr H, Newman AM, Gentles AJ, et al. Role of KEAP1/NRF2 and TP53 mutations in lung squamous cell carcinoma development and radiation resistance. Cancer Discov 2017;7:86–101.
18. Singh A, Bodas M, Wakabayashi N, Bunz F, Biswal S. Gain of Nrf2 function in non-small-cell lung cancer cells confers radioresistance. Antioxid Redox Signal 2010;13:1627–37.
19. McDonald JT, Kim K, Norris AJ, Vlashi E, Phillips TM, Lagadec C, et al. Ionizing radiation activates the Nrf2 antioxidant response. Cancer Res 2010;70:8886–95.
20. Chuang JC, Stehr H, Liang Y, Das M, Huang J, Diehn M, et al. ERBB2-mutated metastatic non–small cell lung cancer: response and resistance to targeted therapies. J Thorac Oncol 2017;12:833–42.
21. Bradley JD, Hu C, Komaki RR, Masters GA, Blumenschein GR, Schild SE, et al. Long-term results of NRG Oncology RTOG 0617: standard- versus high-dose chemoradiotherapy with or without cetuximab for unresectable stage III non–small-cell lung cancer. J Clin Oncol 2020;38:706–14.
22. Taylor MD, Nagji AS, Bhamidipati CM, Theodosakis N, Kozower BD, Lau CL, et al. Tumor recurrence after complete resection for non-small cell lung cancer. Ann Thorac Surg 2012;93:1813–21.
23. Seki A, Rutz S. Optimized RNP transfection for highly efficient CRISPR/Cas9-mediated gene knockout in primary T cells. J Exp Med 2018;215:985–97.
24. Liu J, Lichtenberg T, Hoadley KA, Poisson LM, Lazar AJ, Cherniack AD, et al. An integrated TCGA pan-cancer clinical data resource to drive high-quality survival outcome analytics. Cell 2018;173:400–416.e11.
25. Abazeed ME, Adams DJ, Hurov KE, Tamayo P, Creighton CJ, Sonkin D, et al. Integrative radiogenomic profiling of squamous cell lung cancer. Cancer Res 2013;73:6289–98.
26. Newman AM, Steen CB, Liu CL, Gentles AJ, Chaudhuri AA, Scherer F, et al. Determining cell type abundance and expression from bulk tissues with digital cytometry. Nat Biotechnol 2019;37:773–82.
27. Kim JW, Botvinnik OB, Abudayyeh O, Birger C, Rosenbluh J, Shrestha Y, et al. Characterizing genomic alterations in cancer by complementary functional associations. Nat Biotechnol 2016;34:539–46.
28. Galan-Cobo A, Sitthideatphaiboon P, Qu X, Poteete A, Pisegna MA, Tong P, et al. LKB1 and KEAP1/NRF2 pathways cooperatively promote metabolic reprogramming with enhanced glutamine dependence in KRAS-mutant lung adenocarcinoma. Cancer Res 2019;79:3251–67.
29. Romero R, Sayin VI, Davidson SM, Bauer MR, Singh SX, LeBoeuf SE, et al. Keap1 loss promotes Kras-driven lung cancer and results in dependence on glutaminolysis. Nat Med 2017;23:1362–8.
30. Kitajima S, Ivanova E, Guo S, Yoshida R, Campisi M, Sundararaman SK, et al. Suppression of STING associated with LKB1 loss in KRAS-driven lung cancer. Cancer Discov 2019;9:34–45.
31. Skoulidis F, Goldberg ME, Greenawalt DM, Hellmann MD, Awad MM, Gainor JF, et al. STK11/LKB1 mutations and PD-1 inhibitor resistance in KRAS-mutant lung adenocarcinoma. Cancer Discov 2018;8:822–35.
32. Hamaji M, Chen F, Matsuo Y, Ueki N, Hiraoka M, Date H. Treatment and prognosis of isolated local relapse after stereotactic body radiotherapy for clinical stage I non-small-cell lung cancer: importance of salvage surgery. J Thorac Oncol 2015;10:1616–24.
33. Hast BE, Cloer EW, Goldfarb D, Li H, Siesser PF, Yan F, et al. Cancer-derived mutations in KEAP1 impair NRF2 degradation but not ubiquitination. Cancer Res 2014;74:808–17.
34. Berger AH, Brooks AN, Wu X, Shrestha Y, Chouinard C, Piccioni F, et al. High-throughput phenotyping of lung cancer somatic mutations. Cancer Cell 2016;30:214–28.
35. Caboux E, Paciencia M, Durand G, Robinot N, Wozniak MB, Galateau-Salle F, et al. Impact of delay to cryopreservation on RNA integrity and genome-wide expression profiles in resected tumor samples. PLoS One 2013;8:e79826.
36. Zhang Y, Xiang Y. Molecular and cellular basis for the unique functioning of Nrf1, an indispensable transcription factor for maintaining cell homoeostasis and organ integrity. Biochem J 2016;473:961–1000.
37. Estrela JM, Ortega A, Obrador E. Glutathione in cancer biology and therapy. Crit Rev Clin Lab Sci 2006;43:143–81.
38. LeBoeuf SE, Wu WL, Karakousi TR, Karadal B, Jackson SR, Davidson SM, et al. Activation of oxidative stress response in cancer generates a druggable dependency on exogenous non-essential amino acids. Cell Metab 2020;31:339–350.e4.
39. Meijer TWH, Peeters WJM, Dubois LJ, van Gisbergen MW, Biemans R, Venhuizen JH, et al. Targeting glucose and glutamine metabolism combined with radiation therapy in non-small cell lung cancer. Lung Cancer Amst Neth 2018;126:32–40.
40. Hassanein M, Hoeksema MD, Shiota M, Qian J, Harris BK, Chen H, et al. SLC1A5 mediates glutamine transport required for lung cancer cell growth and survival. Clin Cancer Res 2013;19:560–70.
41. Vanhove K, Derveaux E, Graulus GJ, Mesotten L, Thomeer M, Noben JP, et al. Glutamine addiction and therapeutic strategies in lung cancer. Int J Mol Sci 2019;20:252.
42. Momcilovic M, Bailey ST, Lee JT, Fishbein MC, Braas D, Go J, et al. The GSK3 signaling axis regulates adaptive glutamine metabolism in lung squamous cell carcinoma. Cancer Cell 2018;33:905–921.e5.
43. Boysen G, Jamshidi-Parsian A, Davis MA, Siegel ER, Simecka CM, Kore RA, et al. Glutaminase inhibitor CB-839 increases radiation sensitivity of lung tumor cells and human lung tumor xenografts in mice. Int J Radiat Biol 2019;95:436–42.
44. Singh A, Misra V, Thimmulappa RK, Lee H, Ames S, Hoque MO, et al. Dysfunctional KEAP1-NRF2 interaction in non-small-cell lung cancer. PLoS Med 2006;3:e420.
45. Jeong Y, Hellyer JA, Stehr H, Hoang NT, Niu X, Das M, et al. Role of KEAP1/NFE2L2 mutations in the chemotherapeutic response of non-small cell lung cancer patients. Clin Cancer Res 2020;26:274–81.
46. Goeman F, Nicola FD, Scalera S, Sperati F, Gallo E, Ciuffreda L, et al. Mutations in the KEAP1-NFE2L2 pathway define a molecular subset of rapidly progressing lung adenocarcinoma. J Thorac Oncol 2019;14:1924–34.
47. Iyengar P, Wardak Z, Gerber DE, Tumati V, Ahn C, Hughes RS, et al. Consolidative radiotherapy for limited metastatic non-small-cell lung cancer: a phase 2 randomized clinical trial. JAMA Oncol 2018;4:e173501.
48. Gomez DR, Tang C, Zhang J, Blumenschein GR, Hernandez M, Lee JJ, et al. Local consolidative therapy vs. maintenance therapy or observation for patients with oligometastatic non-small-cell lung cancer: long-term results of a multi-institutional, phase II, randomized study. J Clin Oncol 2019;37:1558–65.
49. Palma DA, Olson R, Harrow S, Gaede S, Louie AV, Haasbeek C, et al. Stereotactic ablative radiotherapy versus standard of care palliative treatment in patients with oligometastatic cancers (SABR-COMET): a randomised, phase 2, open-label trial. Lancet 2019;393:2051–8.

50. Dziedzic DA, Rudzinski P, Langfort R, Orlowski T, Polish Lung Cancer Study Group (PLCSG). Risk factors for local and distant recurrence after surgical treatment in patients with non-small-cell lung cancer. Clin Lung Cancer 2016;17:e157–67.
51. Trakul N, Chang CN, Harris J, Chapman C, Rao A, Shen J, et al. Tumor volume-adapted dosing in stereotactic ablative radiotherapy of lung tumors. Int J Radiat Oncol Biol Phys 2012;84:231–7.
52. Ohri N, Bodner WR, Halmos B, Cheng H, Perez-Soler R, Keller SM, et al. (18)F-fluorodeoxyglucose/positron emission tomography predicts patterns of failure after definitive chemoradiation therapy for locally advanced non-small cell lung cancer. Int J Radiat Oncol Biol Phys 2017;97:372–80.
53. Przybyl J, Chabon JJ, Spans L, Ganjoo KN, Vennam S, Newman AM, et al. Combination approach for detecting different types of alterations in circulating tumor DNA in leiomyosarcoma. Clin Cancer Res 2018;24:2688–99.
54. Gazdar A. Activating and resistance mutations of EGFR in non-small-cell lung cancer: role in clinical response to EGFR tyrosine kinase inhibitors. Oncogene 2009;28:S24–31.
55. Karczewski KJ, Francioli LC, Tiao G, Cummings BB, Alföldi J, Wang Q, et al. Variation across 141,456 human exomes and genomes reveals the spectrum of loss-of-function intolerance across human protein-coding genes. bioRxiv 2019;531210.
56. Srivastava A, Sarkar H, Gupta N, Patro R. RapMap: a rapid, sensitive and accurate tool for mapping RNA-seq reads to transcriptomes. Bioinformatics 2016;32:i192–200.
57. Gentles AJ, Hui ABY, Feng W, Azizi A, Nair RV, Knowles DA, et al. Clinically-relevant cell type cross-talk identified from a human lung tumor microenvironment interactome. bioRxiv 2019;637306.
58. Guzmán C, Bagga M, Kaur A, Westermarck J, Abankwa D. ColonyArea: an ImageJ plugin to automatically quantify colony formation in clonogenic assays. PLoS One 2014;9:e92444.